# Coupling reduced models for optimal motion estimation

Karim Drifi, Isabelle Herlin

# Coupling Reduced Models for Optimal Motion Estimation

Karim Drifi[1,2], Isabelle Herlin[1,2]
[1]*INRIA, Institut National de Recherche en Informatique et Automatique,*
[2]*CEREA, joint laboratory ENPC - EDF R&D*
*Karim.Drifi@inria.fr, Isabelle.Herlin@inria.fr*

## Abstract

*The paper discusses the issue of motion estimation by image assimilation in numerical models, based on Navier-Stokes equations. In such context, models' reduction is an attractive approach that is used to decrease cost in memory and computation time. A reduced model is obtained from a Galerkin projection on a subspace, defined by its orthogonal basis. Long temporal image sequences may then be processed by a sliding-window method. On the first sub-window, a fixed basis is considered to define the reduced model. On the next ones, a Principal Order Decomposition is applied, in order to define a basis that is simultaneously small-size and adapted to the studied image data. Results are given on synthetic data and quantified according to state-of-the-art methods. Application to satellite images demonstrates the potential of the approach.*

## 1. Introduction

Many authors investigate the issue of fluid flow motion estimation and a complete survey can be found for instance in [2]. In this paper, we are interested by the approach of data assimilation using a dynamic equation on the velocity field: motion is estimated as a compromise between that dynamics and image observations [1]. As the memory requirement and computation time of these data assimilation methods are proportional to image size, the issue of reduction arises. We describe, in Section 3, the reduction on a sine basis, whose results are analyzed in Section 5. This reduced model is applicable to estimate motion on a short temporal sequence. In Section 4, processing of long sequences is described with the use of the sine basis on a first short temporal sub-window and of Principal Order Decomposition on the following sub-windows. This is a coupling of reduced models with a sliding-window approach. Results are given in Section 5. The next section, Section 2, describes first the mathematical formalism of the paper and the model used for illustrating the coupling of reduced models.

## 2. Data Assimilation and Model Reduction

To illustrate our approach of model reduction, we consider divergence-free motion fields $\mathbf{w}(\mathbf{x},t)$, with $\mathbf{x} = \begin{pmatrix} x & y \end{pmatrix}^T \in \Omega$, a bounded domain, $t \in [t_0, t_N]$, a closed interval, and $\mathbf{w} = \begin{pmatrix} u & v \end{pmatrix}^T$. We assume that the motion field satisfies the heuristics of Lagrangian constancy described by: $\frac{d\mathbf{w}}{dt} = \frac{\partial \mathbf{w}}{\partial t} + (\mathbf{w} \cdot \nabla)\mathbf{w} = 0$. This is rewritten as an equation on the evolution of the vorticity $\xi$ under the divergence-free assumption:

$$\frac{\partial \xi}{\partial t} + \mathbf{w}(\xi) \cdot \nabla \xi = 0 \tag{1}$$

We consider a variable $I_s$, named pseudo-image, which has the same dynamics than the image observation: the motion field transports it according to:

$$\frac{\partial I_s}{\partial t} + \mathbf{w}(\xi) \cdot \nabla I_s = 0 \tag{2}$$

This pseudo-image is included in the state vector in order to allow an easy comparison with image observations at acquisition dates: they have to be almost identical. The state vector of the model is then defined as $\mathbf{X}(\mathbf{x},t) = \begin{pmatrix} \xi(\mathbf{x},t) & I_s(\mathbf{x},t) \end{pmatrix}^T$, and Eqs. 1 and 2 are summarized as:

$$\frac{\partial \mathbf{X}}{\partial t} + \mathbb{M}(\mathbf{X}) = 0 \tag{3}$$

Data assimilation aims to find an optimal solution to the evolution equation (Eq. 3) and to the observation equation that links the state vector, in fact its pseudo-image component $I_s$, to image observations $I(\mathbf{x},t)$:

$$I_s = I \tag{4}$$

Images are assimilated in the Full Model (FM), $\mathbb{M}$, in order to estimate vorticity and motion. Detailed description of the data assimilation method is given in [1].

In order to obtain a reduced model of $\mathbb{M}$, subspaces for vorticity fields and pseudo-images have to be chosen, defined by their respective orthogonal basis $\Phi$ and $\Psi$. Let $a_i(t)$ and $b_j(t)$ be the projection coefficients of $\xi(\mathbf{x},t)$ and $I_s(\mathbf{x},t)$ on $\Phi$ and $\Psi$, it comes: $\xi(\mathbf{x},t) \approx \sum_{i=1}^{K} a_i(t)\phi_i(\mathbf{x})$ and $I_s(\mathbf{x},t) \approx \sum_{j=1}^{L} b_j(t)\psi_j(\mathbf{x})$. After replacing in Eqs. 1 and 2, simplifying the equations, and using the property that $\mathbf{w}$ is a linear function of $\xi$, it comes:

$$\begin{cases} \dfrac{da_k}{dt}(t) + a^T(t)B(k)a(t) = 0, \quad k = 1 \dots K. \\ \dfrac{db_l}{dt}(t) + a^T(t)G(l)b(t) = 0, \quad l = 1 \dots L. \end{cases} \tag{5}$$

with:

- $a(t) = \begin{pmatrix} a_1(t) & \dots & a_K(t) \end{pmatrix}^T$,
- $b(t) = \begin{pmatrix} b_1(t) & \dots & b_L(t) \end{pmatrix}^T$,
- $B(k)$ a $K \times K$ matrix: $B(k)_{i,j} = \dfrac{\langle \mathbf{w}(\phi_i) \cdot \nabla\phi_j, \phi_k \rangle}{\langle \phi_k, \phi_k \rangle}$,
- $G(l)$ a $K \times L$ matrix: $G(l)_{i,j} = \dfrac{\langle \mathbf{w}(\phi_i) \cdot \nabla\psi_j, \psi_l \rangle}{\langle \psi_l, \psi_l \rangle}$
- $\langle ., . \rangle$ the scalar product: $\langle f, g \rangle = \int f(\mathbf{x})g(\mathbf{x})d\mathbf{x}$,
- $\mathbf{w}(\phi_i)$ the motion field associated with the vorticity field $\phi_i$.

Let $\mathbf{X}_R(\mathbf{x},t) = \begin{pmatrix} a(t)^T & b(t)^T \end{pmatrix}^T$ be the state vector of the reduced model. System 5 is rewritten as:

$$\frac{d\mathbf{X}_R}{dt} + \mathbb{M}_R(\mathbf{X}_R) = 0 \tag{6}$$

$\mathbb{M}_R$ is the Galerkin projection of the full model $\mathbb{M}$ on $\Phi$ and $\Psi$.

## 3. Sine Basis

A sine basis $\Phi$ is chosen to define the vorticity subspace, whose element $i$ is:

$$\phi_i = \phi_{(i_1,i_2)} = \begin{pmatrix} \sin(\pi i_1 h_x) sin(\pi i_2 h_y) \\ \dots \\ \sin(N_x \pi i_1 h_x) sin(\pi i_2 h_y) \\ \sin(\pi i_1 h_x) sin(2\pi i_2 h_y) \\ \dots \\ \sin(N_x \pi i_1 h_x) sin(2\pi i_2 h_y) \\ \dots \\ \sin(\pi i_1 h_x) sin(N_y \pi i_2 h_y) \\ \dots \\ \sin(N_x \pi i_1 h_x) sin(N_y \pi i_2 h_y) \end{pmatrix}$$

with:

- $i = (i_1, i_2)$ a double index,
- $h_x = \dfrac{1}{N_x + 1}$, $N_x$ image size in direction $x$,
- $h_y = \dfrac{1}{N_y + 1}$, $N_y$ image size in direction $y$.

$\phi_i$ is an eigenvector of the Laplace operator $\Delta$ associated to the eigenvalue

$$\lambda_i = -2[2 - \cos(\pi i_1 h_x) - \cos(\pi i_2 h_y)] \times \frac{1}{d^2} \tag{7}$$

$d$ being the pixel resolution in both directions $x$ and $y$. To compute $\mathbf{w}(\phi_i)$, we use this eigenvector property and derive the stream function $\varphi_i$ that is solution of the Poisson equation:

$$\Delta\varphi_i = \phi_i \tag{8}$$

We have $\varphi_i = \phi_i/\lambda_i$ and $\mathbf{w}(\phi_i)$ is then derived from $\varphi_i$ by:

$$\mathbf{w} = \begin{pmatrix} -\frac{\partial\varphi_i}{\partial y} & \frac{\partial\varphi_i}{\partial x} \end{pmatrix}^T \tag{9}$$

A Sine Reduced Model (SRM) is obtained by applying the Galerkin projection to the full model, defined by Eq. 3: vorticity is projected on $\Phi$ and pseudo-image is projected on itself (no reduction). As vorticity and motion are weighted sums of the sine functions, the result has the same spatial properties. In particular, the result is smooth, which is of major interest if image observations are noisy. This is a major advantage of SRM. However, this model has the same size as the full model if the full basis $\Phi$ is used. In this case, it offers no gain in memory size and computation time.

## 4. Sliding Windows

Having obtained the reduced model SRM for processing short temporal image sequences, the issue of processing long time intervals arises, which is solved by the sliding-window method.

The discrete sequence $I = \{I^z\}_{z=1\dots Z}$ is first split into short sub-sequences, for instance 4 images, that half overlap in time. The corresponding temporal intervals or windows are denoted $W_m$, with $m$ being their index. Images belonging to $W_1$ are assimilated in SRM. This allows the retrieval of the vorticity on $W_1$. Its value at the beginning of $W_2$ is taken as initial condition for a simulation by the full model of Eq. 3. Principal Order Decomposition (POD) is then applied to the simulated sequences of vorticity $\xi$ and pseudo-image $I_s$ in order to generate bases $\Phi$ and $\Psi$ and obtain a reduced model, named POD-POD Reduced Model of the 2nd window (PPRM2). The coefficients of projection of images belonging to $W_2$ are assimilated in PPRM2 to retrieve the vorticity coefficients and compute the vorticity values over $W_2$. This again provides the initial condition

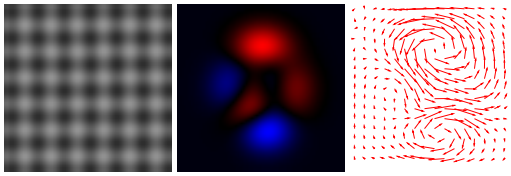

**Figure 1. Pseudo-image, vorticity and motion field at $t = 0$. Positive vorticity values are red and negative one blue.**

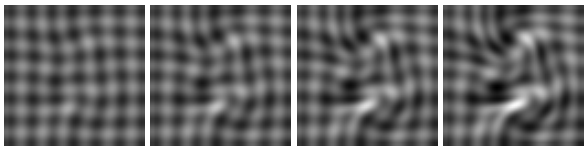

**Figure 2. Four observations.**

for $W_3$ and allows to define a new POD-POD Reduced Model on the third window (PPRM3). The process is then iterated until the whole image sequence $I$ has been analyzed.

The major advantage of this approach is that assimilation in the Sine Reduced Model is only applied on the first temporal window $W_1$, that has short duration. On the next windows $W_m$, the complexity greatly decreases, as the state vectors involved in the POD-POD Reduced Models are of size less than 10 in the experiments.

## 5. Results

Results of the Sine Reduced Model are first provided on synthetic and satellite images. Then the sliding-window method is tested on synthetic data in order to demonstrate the potential of the method to process long temporal windows.

The divergence-free model is run from the initial conditions displayed in Figure 1. This provides a sequence of five observations (the first one is the initial condition and the next four are displayed on Figure 2) and the ground-truth of vorticity and motion over the whole temporal domain. Assimilation experiments are performed with these five observations in order to retrieve the vorticity and motion fields with the Full Model and the Sine Reduced Model. For these experiments, the background of vorticity (FM) or vector $a$ (SRM) is set to zero and the one of pseudo-image is the first observation. The result of the assimilation process is the state vector $\mathbf{X}(k) = \begin{pmatrix} \xi(k) & I_s(k) \end{pmatrix}^T$ and its associated motion vector $\mathbf{w}(k)$ over the same temporal interval than the image sequence. In Table 1, the error

**Table 1. Error analysis: misfit between motion results and ground truth.**

| Method | Ang. err. (in deg.) Mean | Ang. err. (in deg.) Std. Dev. | Relative norm err. Mean (in %) |
|---|---|---|---|
| Horn[3] | 15.26 | 9.65 | 45.75 |
| Papadakis [5] | 13.89 | 5.03 | 45.59 |
| Isambert [4] | 10.61 | 6.92 | 34.84 |
| Suter[7] | 10.41 | 5.34 | 37.65 |
| Sun [6] | 8.76 | 4.26 | 29.07 |
| FM | 0.18 | 0.10 | 0.06 |
| SRM | 1.53 | 1.10 | 0.65 |

between the motion result and the ground truth is given for the Full Model, the Sine Reduced Model and five known state-of-the-art methods. For these five methods, optimal parameter values have been used. Four of them are image processing methods, that rely on $L_2$ regularization of motion [3, 6] or on a second-order regularization of the divergence [4, 7]. These methods are said static, as they do not use any model of motion evolution. Moreover, we compare with [5], that also applies data assimilation for a divergence-free model: the state vector reduces to vorticity and the observation equation is the optical flow equation. Results demonstrate the quality of the Full Model on this so-called twin experiment, and its efficient approximation by the Sine Reduced Model.

The approach is furthermore applied on satellite data. Observations are images acquired by NOAA/AVHRR sensors over Black Sea [1], and measure the Sea Surface Temperature (SST) with a spatial resolution of about 1 km at nadir. In the upper layer of Black Sea, horizontal motion is around 30 $^{cm}/_{s}$ for mesoscale eddies, while vertical motion is around $10^{-4}$ $^{cm}/_{s}$ and can be neglected. The 2D divergence-free assumption is then roughly verified and the Full Model and Sine Reduced model are applicable. The sequence has four observations (see two of them on Figure 3). The results of motion estimation with FM and SRM are displayed on the same figure. Visualisation is made with the coloured representation tool of the Middlebury database [2]. On these coloured images, the orientation and norm of velocity are respectively represented by hue (colour) and saturation.The data assimilation methods also compute the pseudo-image values, that achieve the best compromise between dynamics and observations. At acquisition dates, these pseudo-images are not exactly equal

[1] Data have been provided by E. Plotnikov and G. Korotaev from the Marine Hydrophysical Institute of Sevastopol, Ukraine.

[2] http://vision.middlebury.edu/flow/

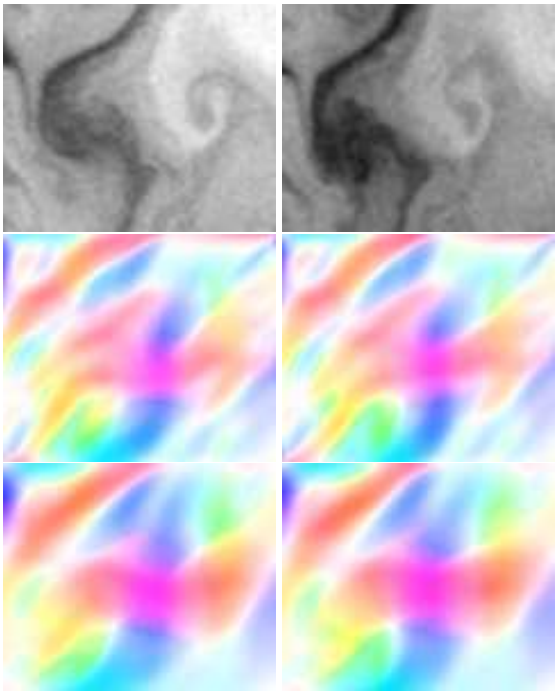

**Figure 3. Observations (top), FM (middle), SRM (bottom) at $t = 1$ (left) and 3 (right).**

**Table 2. Correlation between pseudo-images and observations.**

| Date | 1 | 2 | 3 | 4 |
|---|---|---|---|---|
| FM | 0.99 | 0.93 | 0.94 | 0.97 |
| SRM | 0.99 | 0.94 | 0.94 | 0.96 |

to the observed images. Their correlation measures if the structures (edges) are correctly assessed and if motion is accurately estimated. Correlation results of FM and SRM are given in Table 2: values are close to 1, proving that the motion retrieved by both models are coherent with the dynamics underlying the evolution displayed by the observations. This also points out the performance of SRM. Another mathematical criteria is the RMSE between estimations of vorticity by FM and SRM. Its value is 0.01, which proves that SRM is a good approximation of FM.

The sliding-window method described in Section 4 is then applied on a sequence of 19 image observations, obtained from a run of the Full Model with initial conditions of Figure 1. The discrete sequence is split in 7 windows of five images. The first five observations of $W_1$ are assimilated in SRM. The result is used to define the POD-POD Reduced Model (PPRM2) of $W_2$. The five observations of $W_2$ are then assimilated in PPRM2 and so on until the end of the studied sequence. Comparison of estimated vorticity with ground-truth gives that the RMSE ranges from 0.0016 on $W_2$ to 0.005 on $W_7$, which demonstrates the robustness obtained by coupling the Sine Reduced Model with the coupled POD-POD Reduced Models.

## 6. Conclusions

The paper describes an approach for coupling reduced models and optimally estimate motion on long temporal image sequences. One of these reduced models is the Sine Reduced Basis, which uses a fixed basis and presents smoothness properties. Its results have been quantified and compared to state-of-the-art methods. The second reduced model is the Pod-Pod Reduced Model, which relies on Principal Order Decomposition. Its state vector has a small size, less than 10 in experiments, that allow processing long sequences in almost real time.

## 7. Acknowledgements

Research has been partly funded by the ANR project Geo-FLUIDS (ANR 09 SYSC 005 02).

## References

[1] D. Béréziat and I. Herlin. Solving ill-posed image processing problems using data assimilation. *Numerical Algorithms*, 56(2):219–252, Feb. 2011.

[2] D. Heitz, E. Mémin, and C. Schnörr. Variational fluid flow measurements from image sequences: synopsis and perspectives. *Experiments in Fluids*, 48(3):369–393, 2010.

[3] B. Horn and B. Schunk. Determining optical flow. 17:185–203, 1981.

[4] T. Isambert, I. Herlin, and J.-P. Berroir. Fast and stable vector spline method for fluid flow estimation. In *Proceedings of International Conference on Image Processing*, pages 505–508, 2007.

[5] N. Papadakis, T. Corpetti, and E. Mémin. Dynamically consistent optical flow estimation. In *Proceedings of International Conference on Computer Vision*, pages 1–7, 2007.

[6] D. Sun, S. Roth, and M. Black. Secrets of optical flow estimation and their principles. In *Proceedings of European Conference on Computer Vision*, pages 2432–2439, 2010.

[7] D. Suter. Motion estimation and vector splines. In *Proceedings of Conference on Computer Vision and Pattern Recognition*, pages 939–942, 1994.